

Theoretical and Experimental Studies of Different Amine Compounds as Corrosion Inhibitors for Aluminum in Hydrochloric Acid

Rageh.K. Hussein¹ , Mortaga Abou-Krishna^{2,3}, Tarek A. Yousef^{3,4,*} 

¹ Department of Physics, College of Science, Imam Mohammad Ibn Saud Islamic University (IMSIU), Riyadh 11623, KSA; rahusseini@imamu.edu.sa (R.K.H.);

² Department of Chemistry, Faculty of Science, South Valley University, Qena, 83523, Egypt; m_abou_krishna@yahoo.com (M.A.K.);

³ Department of chemistry, College of Science, Imam Mohammad Ibn Saud Islamic University (IMSIU), Riyadh 11623, KSA; tayousef@imamu.edu.sa (T.A.Y.);

⁴ Department of Toxic and Narcotic drug, Forensic Medicine, Mansoura Laboratory, Medicolegal Organization, Ministry of Justice, Egypt

* Correspondence: tayousef@imamu.edu.sa;

Scopus Author ID 36562771600

Received: 16.07.2020; Revised: 6.09.2020; Accepted: 10.09.2020; Published: 16.09.2020

Abstract: Density Functional Theory investigations using the B3LYP/6-31G* model have been carried out. Several quantum chemical parameters have been computed to interpret the inhibition activity of 2, 4-dinitrophenylhydrazine, o-phenylenediamine, and hydrazine hydrate. The ranking of the quantum chemical calculations classifies 2, 4-Dinitrophenylhydrazine as high efficient inhibitor among the studied molecules. The correspondence of the lowest energy gap ($\Delta E = 4.27$ eV) for the calculated value (88.9%) of the highest inhibition efficiency (%IE) of 2, 4 Dinitrophenylhydrazine. Therefore, in parallel, the experimental inhibition of aluminum corrosion was tested using amine compounds in 1M hydrochloric acid solution by means of gravimetry and gasometry measurements. These compounds have been found to act as effective corrosion inhibitors for aluminum in the acid solution, and the best one was 2, 4-dinitrophenylhydrazine, represent one of the salient agreements between experimental and theoretical measurements. The data are showing that this inhibitor is appropriate for Langmuir adsorption isotherm. SEM micrographs indicate that the surface coverage increases in the presence of 0.5 mM of 2, 4-dinitrophenylhydrazine inhibitor, which in turn results in the formation of the adsorbed compound on the metal surface and the surface is covered by an inhibitor layer that effectively controls the dissolution of aluminum.

Keywords: 2,4-dinitrophenylhydrazine; o-phenylenediamine; hydrazine hydrate; Aluminum Corrosion, Density Functional Theory.

© 2020 by the authors. This article is an open-access article distributed under the terms and conditions of the Creative Commons Attribution (CC BY) license (<https://creativecommons.org/licenses/by/4.0/>).

1. Introduction

Corrosion is a common natural phenomenon that can be chemical or electrochemical in essence, and it degrades the properties of the metal and its alloys, making them unusable. Depending on the roughness of the aluminum surface, the color varying from silvery to medium gray, aluminum is a smooth, strong, lightweight, malleable metal and is non-magnetic and matte. Aluminum and its alloys are used in numerous factories and heavily contaminated areas for building purposes and numerous interior appliances. Due to its low density and its potential to withstand corrosion to some degree owing to the passivation effect, aluminum is remarkable

but its corrosion often happens under aqueous acidic environments. Corrosion of aluminum and its alloys has been thoroughly studied in acidic solutions [1-3]. Several chemicals are commonly used as corrosion inhibitors in the industry to stop or lower the incidence of metal corrosion in an acid medium.

Solutions of hydrochloric acid are typically used in aluminum pickling and electrochemical drilling operations, which usually lead to major metal loss due to corrosion [4,5]. Among numerous ways to protect aluminum from acid corrosion, the most effective and practical method [6,7] to slow down corrosion processes is the addition of organic corrosion inhibitors to the metal's environment. The adsorption [8,9] of such compounds is said to be determined by the electronic structure of the donor site's inhibitory molecules, the steric factor, aromaticity and electron densities, the functional group, and also the polarisability of the group. Previous research indicated that heterocyclic compounds [10] are used as inhibitors of corrosion due to the existence of various adsorption centers (O, N, S, P, and π electrons) that can help form metal ion complexes.

Computational chemistry methods implemented in computer hardware and software have become a noteworthy tool in explaining, characterizing materials and chemical reactions. One of these methods is density functional theory (DFT), which has been broadly applied in many corrosion studies [11-13]. In DFT, calculated quantum chemical parameters were utilized to identify the characteristics of the inhibitor activities in the corrosion mechanism and analyze the interaction between inhibitor and metal surface [14-18]. Such quantum chemical parameters involve the highest occupied molecular orbital (HOMO) energy, the lowest unoccupied molecular orbital (LUMO), the (EHOMO-ELUMO) energy gap, dipole moment, the electronegativity (χ), the global hardness (η), the softness (σ), the charge on the reactive center and other parameters that are used in demonstrating the electronic properties of molecules [19]. The inhibiting activity of CIE(CIE) to the dissolution of Al in 2M HCl medium was carried out by Abd El-Aziz S. Fouda. *et al.* [20]. Moreover, DFT investigations with a 6-31G (d, p) basis set were performed by Diki N *et al.* in order to interpret act out cefadroxil inhibition on aluminum in 1 M solution of hydrochloric acid [21]. The local reactivity of these inhibitors has been evaluated through Mulliken population calculations to illustrate reactive sites for the adsorption process. Potentiodynamic polarization and electrochemical impedance spectroscopy results showed that NBL is a mixed-type corrosion inhibitor of AA7075-T7351 in 1 M HCl environment, which was achieved through the blockage/obstruction/reduction of charge flow by the polymeric barrier on the aluminum alloy's surface [22]. N. Nnaji *et al.* describe the adsorption behavior of organic inhibitors at the aluminum-HCl solution interface, and their corrosion inhibition performance and quantum chemical parameters corroborate well with experimental findings [23]. Also, it has been proven in many research works that O, N, S, P ions, and heterocyclic groups enhance the inhibition efficiency of the molecular structure [24]. This is due to the consideration of these ions as active spots, which facilitates the charge transfer and forming a stable bond between inhibitor and mild steel surface Moretti *et al.* [25].

The theoretical calculation is extremely important because it is trusted results and cheaper than experimental work. Theoretical calculation predicts the result without potential and time consuming; it has high economic value. Still, it is important to prove that these theoretical results were obtained through simple experimental results. There are many papers on the use of amines compounds as corrosion inhibitors, but the literature on computational simulation of molecular structure and theoretical calculations parameters of these compounds as corrosion inhibitors of aluminum in HCl are very few. Therefore, in this research, the authors

directed the work to make the comparison between these compounds as corrosion inhibitors for aluminum in hydrochloric acid from the point of view of the computational simulation of molecular structure and the electronic energies parameters and then theoretically prove by the experimental results using gravimetric and gasometrical methods.

In this work, three different amine compounds named as 2,4-Dinitrophenylhydrazine, o-phenylenediamine, and Hydrazine Hydrate have been examined as corrosion inhibitors for aluminum in hydrochloric acid. Both experimental and theoretical techniques have been used throughout this study. From a theoretical point of view, quantum chemical calculation represented in the DFT method, including B3LYP - 6-31G (d,p) model, was conducted to evaluate the mentioned molecules as corrosion inhibitors. In parallel with the theoretical study, the experimental section gasometry and weight loss measurements have been applied to obtain the inhibition efficiency.

2. Materials and Methods

2.1. Computational details.

The amino compounds referred to by DFT performed using Lee-Yang-Parr (B3LYP) were analyzed using the Becke Three Parameter Hybrid Functional method. [26,27]. 6-31G* has been utilized in the calculations as the basis set the calculated quantum chemical parameters always employed in the analysis of the mechanisms of the inhibitor characteristics and structural nature description of the inhibitor on the corrosion process Ebenso *et al.* [28]. All optimization calculations were done by using Orca 4.0.0 quantum chemistry program package Neese [29]. Both optimized structures draw, and results in visualization was done by using Avogadro 1.2.0n molecular editor program Hanwell *et al.* [30].

The inhibition behavior of organic compounds can be explained by some theoretical correlations known as quantum chemical parameters. Koopman's theorem [31,32] expressed these quantities in series of approximations as follow:

$$I = -E_{HOMO} \quad (1)$$

$$A = -E_{LUMO} \quad (2)$$

$$\chi = -\frac{(E_{HOMO}+E_{LUMO})}{2} = \frac{I+A}{2} \quad (3)$$

$$\eta = -\frac{(E_{HOMO}-E_{LUMO})}{2} = \frac{I-A}{2} \quad (4)$$

$$\sigma = \frac{1}{\eta} = -\frac{2}{(E_{HOMO}-E_{LUMO})} \quad (5)$$

$$\omega = \frac{\chi^2}{2\eta} \quad (6)$$

$$N_{MAX} = \frac{\chi}{\eta} \quad (7)$$

Where E_{HOMO} is the highest occupied molecular orbital energy, E_{LUMO} the lowest unoccupied molecular orbital energy, (χ) is electronegativity, (A) is electron affinity, (η) is global hardness, (σ) is softness, (I) is ionization potential, (ω) is electrophilicity index and (ΔN) is the fraction of electron transferred.

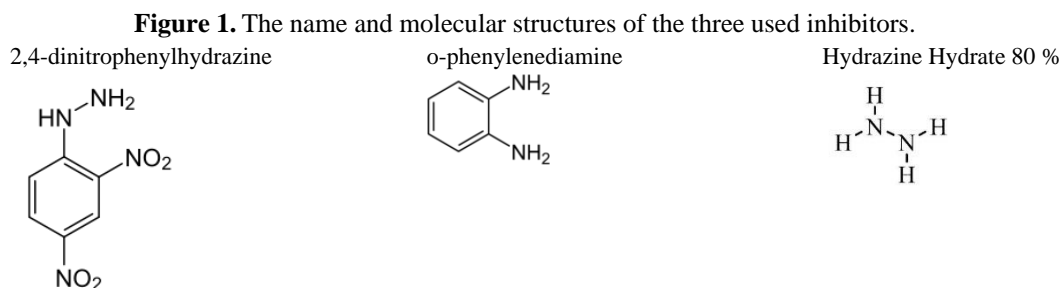
2.2. Aluminum specimen.

The samples used in this study were collected from aluminum at 99.99%. For the Gravimetric method 4 cm x 1.3 cm x 0.13 cm rectangular aluminum samples and for the Gasometry method 3 cm x 0.6 cm x 0.13 cm is used. The specimens were degreased before

each run using a solution containing Na_2CO_3 (25 g/L), Na_3PO_4 (25 g/L), and a wetting agent (synthetic detergent with the active ingredient dodecylbenzene sulphonate) (10 g/L) for 2 minutes at 85.0°C , then washed with distilled water and dipping in a pickling solution (4 M HCl) for one minute followed by hot and cold distilled water.

2.3. Reagents.

From Sigma-Aldrich Chemicals, 2,4-dinitrophenylhydrazine, o-phenylenediamine, and 80 % hydrazine hydrate obtained and used as an inhibitor (Figure 1). A 37% hydrochloric acid solution analytical grade from Merck Chemicals was used to prepare corrosive aqueous solutions.



2.4. Solution preparation.

The blank, a 1 M HCl solution, was prepared by using double distilled water to dilute the concentrated hydrochloric acid. 1 M HCl with an inhibitor solution was prepared at concentrations of 4-10 mM.

2.5. Experimental methods.

2.5.1. Gravimetric measurements.

A 100 ml beaker holding 50 ml of test solution was used for gravimetric measurements. At 298 K, the 24 hours immersion time was used to weight loss method. Three simultaneous experiments were conducted to obtain repeatable good results, and average weight loss was used to calculate the corrosion rates (CR) are calculated based on the weight loss (WL) measurement as the following equation (Eq. 8):

$$\text{CR} = \text{WL}/(\text{A}_s \times t). \quad (8)$$

Where A_s is the sample surface area in cm^2 , t is the immersion time in hours (hrs), WL is the weight loss in mg. The inhibition efficiency (IE) is calculated by the equation (Eq. 9) as follows:

$$\text{IE}(i) = 100 \times [\text{CR}(0) - \text{CR}(i)] / \text{CR}(0). \quad (9)$$

Where $\text{CR}(0)$ is the corrosion rate of HCl solution without inhibitors in $\text{mg} \cdot \text{cm}^{-2} \cdot \text{h}^{-1}$; $\text{CR}(i)$ is the corrosion rate of HCl solution with a certain amount of inhibitor in $\text{mg} \cdot \text{cm}^{-2} \cdot \text{h}^{-1}$.

The degree of surface coverage (Θ) and the inhibition efficiency (IE) using Equation 3:

$$\Theta = [\text{CR}(0) - \text{CR}(i)] / \text{CR}(0). \quad (10)$$

2.5.2. Gasometry method.

The progression of the corrosion reaction was calculated by the volumetric calculation of the hydrogen being produced. Corrosion rate r (mL min^{-1}) was taken as a straight line slope reflecting the increase in the quantity of hydrogen and the period of exposure.

IE , inhibition efficiency was calculated by using equation 11:

$$IE = [1 - (r / r_0)] \times 100 \quad (11)$$

where r and r_0 are the aluminum sample corrosion rates in the presence and absence of the utilized inhibitor.

Degrees of surface coverage (θ) with various inhibitors were evaluated from data of weight loss:

$$\theta = [1 - (r / r_0)]. \quad (12)$$

2.6. Adsorption isotherm.

Adsorption isotherm Ayawei [33] can be calculated by supposing that the inhibition effect is mainly due to adsorption in an interface between metal/solution. Specific details about the inhibitor adsorption may be given by isothermal adsorption on the metal sheet. To achieve the isotherm, the fractional coverage values (θ) must be calculated as a function of the concentration of the inhibitor. It is, therefore, important to empirically evaluate which isotherm is better fitted to inhibitor adsorption on the aluminum surface.

To research the association (adsorption mechanism) between the metal (aluminum) and the inhibitor molecules, various isotherms of adsorption have been studied. The adsorption meets the Freundlich adsorption isotherm by providing a strong correlation coefficient if it obeys the following equation:

$$\text{Freundlich Isotherm} \quad \log \theta = \log K + 1/n \log C \quad (13)$$

Another isotherms tested, and the equation used is Langmuir Isotherm

$$C/\theta = 1/K + C \quad (14)$$

Where C = concentration, θ = Degree of surface coverage, K and n are constants

2.7. Surface characterization.

The Hitachi S-3000 computer-operated Scanning Electron Microscope was used to research the morphology of the aluminum surface in the presence or absence of a tested inhibitor at room temperature for 24 h immersion.

3. Results and Discussion

3.1. Quantum calculations results.

Figure 2 demonstrates the optimized molecular structures for the substances being studied. Table 1 describes the values of various quantum chemical parameters such as E_{HOMO} , E_{LUMO} , energy gap ΔE ($E_{HOMO} - E_{LUMO}$), the number of transferred electrons (ΔN), global hardness (η), softness (σ), dipole moment (μ) and electronegativity (χ).

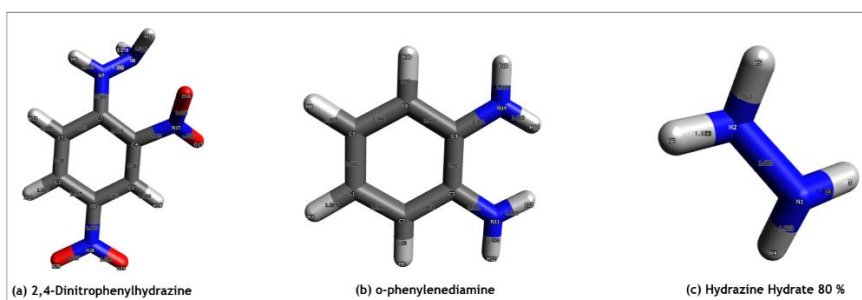


Figure 2. Optimized structure of studied molecules.

Table 1. The studied inhibitors' calculated Quantum chemical descriptors.

	E _{HOMO} (eV)	E _{LUMO} (eV)	ΔE (eV)	IP	EA	μ (Debye)	χ	η	σ	ΔN _{max}	ω
2,4-Dinitrophenylhydrazine	-6.73	-2.46	4.27	6.73	2.46	8.21	4.60	2.14	0.47	2.15	4.94
o-phenylenediamine	-4.35	0.92	5.27	4.35	-0.92	3.01	1.72	2.64	0.38	0.65	0.56
Hydrazine Hydrate 80 %	-5.34	2.18	7.52	5.34	-2.18	0.00	1.58	3.76	0.27	2.42	0.33

The frontier molecular orbital theory describes the E_{HOMO} as it owns the ability to donate an electron to apposite electron acceptors, while the molecule's ability to accept an electron is relevant to E_{LUMO} [34,35]. Furthermore, the higher value of E_{HOMO} is believed to grant higher inhibition efficiency for a molecule. Also, good inhibition efficiency is associated with a molecule with the lower value of E_{LUMO} [36,37]. From Table 1, one can see that o-phenylenediamine has the highest HOMO energy while 2, 4-dinitrophenylhydrazine has the lowest LUMO energy, which reflects a desirable characteristic for the two compounds as inhibitors.

A. Kosari *et al.* [37] established previously that the smaller value of ΔE corresponding to high chemical reactivity and higher inhibition performance. As indicated in Table 1, the values of ΔE revealed that 2,4-Dinitrophenylhydrazine has the smallest HOMO-LUMO gap (4.27 eV) and is the best inhibitor. The dipole moment μ is a relevant descriptor for the inhibition activity of molecular structure. High inhibition efficiency is correlated with a higher value of dipole moment Behpour *et al.* [38].

The dipole moment of the studied three molecules in Table 1 has the order: 2,4-Dinitrophenylhydrazine > o-phenylenediamine > Hydrazine Hydrate 80, which highlights the high ability of 2,4-Dinitrophenylhydrazine to be adsorbed on the metal surface.

Electronegativity is the chemical potential that measures how strongly electrons are attracted to molecules. A molecule with a higher value of electronegativity χ shows better inhibition properties Parr *et al.* [39]. The higher value of χ in Table 1 was recorded for 2, 4-Dinitrophenylhydrazine, making it the best inhibitor performance among the studied molecules. Hardness (η) and softness (σ) are two notable parameters to understand the stability and reactivity of organic compounds. The resistance of molecule or atom to charges transfer during a chemical reaction is defined as chemical hardness, while softness determines the capacity of a molecule or atom to receive electrons. The metal surface demonstrates a higher inhibition efficiency if it has the smallest value of hardness or the highest value of softness [40,41]. In Tables 1, 2, 4-Dinitrophenylhydrazine has the lowest hardness value (2.14), highest softness value (0.47), giving it the highest probability to bind on metal surfaces and form a good protecting inhibitor.

The number of transferred electrons (ΔN) is another indication for the efficiency of corrosion inhibition, expressing the molecule capability to donate electrons for metal surface. The molecule, which has the highest value of (ΔN), is viewed as a good inhibitor that having the highest potential to interact with the metal surface. If the range of the number of transferred electrons (ΔN) < 3.6, then the molecule which has the highest value of (ΔN) is viewed as a good inhibitor that having the highest potential to interact with the metal surface Lukovits *et al.* [42]. As it is obvious in Table 1, the highest value of (ΔN) was observed for 2,4-Dinitrophenylhydrazine, which documented the priority of 2,4-Dinitrophenylhydrazine as a stronger inhibitor than o-phenylenediamine and Hydrazine Hydrate 80 %.

The electrophilicity index ω determines the strength of the adsorption of the inhibitor on the metal surface by measuring the inhibitor capacity to receive electrons from the metal surface. A strong inhibitor is remarkable, with a high value of electrophilicity. As depicted in

Table 1, the 2,4-Dinitrophenylhydrazine shows the highest value (4.94) of electrophilicity. Thus, it can be inferred that 2, 4-Dinitrophenylhydrazine is the most effective inhibitor in the course of our study.

The distributions of HOMO and LUMO frontier molecular orbitals provide details about energetic sites in molecules. HOMO orbitals describe the regions which have the ability to donate electrons to acceptor regions with empty low energy orbital. The LUMO orbitals are associated with regions with the capacity of accepting electrons. The frontier molecule orbitals of studied compounds are illustrated in Figure. 3. In 2, 4-Dinitrophenylhydrazine, the HOMO mainly consists of bonding orbitals cover the C=C-C group in benzene ring beside small phases located over oxygen atoms and the upper nitrogen atom, whereas LUMO is antibonding orbitals spread over the whole molecule. In o-phenylenediamine, HOMO delocalized over three phases C=C-C=C group, C=C bond, and the two nitrogen atoms while LUMO in the region including C-C, C=C, and C-H bonds in the benzene ring. In Hydrazine Hydrate 80 %, there are two HOMO phases surrounding the two H-N-H bonds, while the ambiguous LUMO phase surrounding the molecule as indicated by the line view in Figure 3. Therefore, these sites are representing active spots for the probable electrons transfers in reactions mechanism of between inhibitors and metal surfaces.

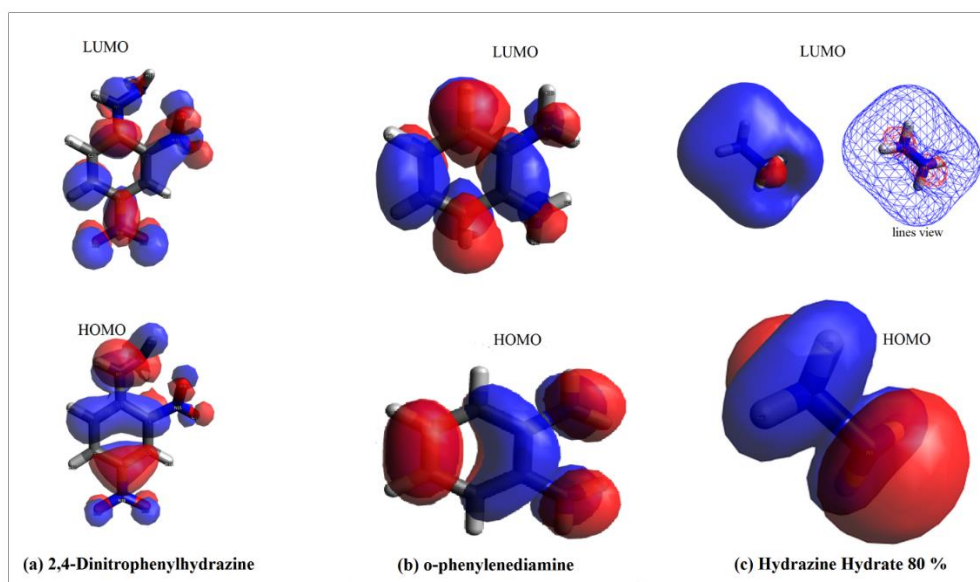


Figure 3. Frontier molecular (HOMO - LUMO) diagram.

The selectivity of chemical inhibitors depends on the partial atomic charges on the atoms of the molecules. For example, if the metal surface is Al, which has a positive charge in acidic solution, then the inhibitor molecules with the highest negative charge atoms have the highest tendency to be adsorbed on the Al metal surface. In Figure 4, the calculated Mulliken atomic charges are clarified on the optimized geometries of the investigated molecules. 2,4-Dinitrophenylhydrazine containing the majority of negative charge atoms identified on oxygens and some of carbon and nitrogen atoms. The highest negative charge (-0.84) on two nitrogen atoms in o-phenylenediamine turned to a positive charge (0.39) in 2,4-Dinitrophenylhydrazine due to bonded to (pulling electrons) oxygen atoms. There are only two intermediate negative charge carriers (nitrogen atoms) in Hydrazine Hydrate 80 %. The charges distribution in Hydrazine Hydrate 80 % (equal and opposite vectors of bond dipoles) clarifies the zero value of dipole moment indicated in Table 1.

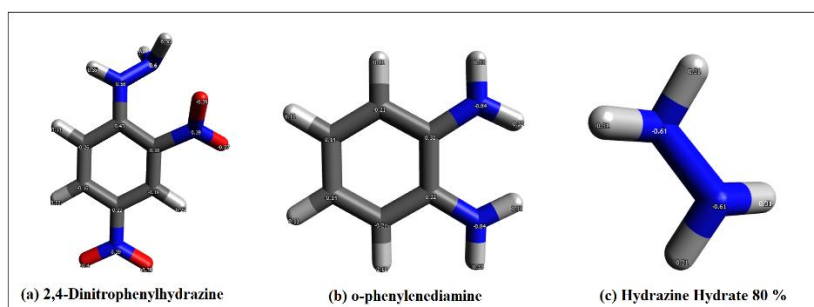


Figure 4. Mulliken charges are illustrated on the optimized structure of studied molecules.

3.2. Gravimetric measurements.

Table 2 summarizes the percentage of inhibition efficiency (% I E) and fractional surface coverage values (θ) obtained from the process of weight loss for different inhibitors (0.02 mM) in 1 M HCl.

From the above findings, it is obvious that the strongest inhibitor was 2, 4-dinitrophenylhydrazine and the %IE for various compounds investigated decreases in the following order: 2, 4-dinitrophenylhydrazine > o-phenylenediamine > hydrazine hydrate.

The above order maybe because dinitro phenylhydrazine has more donor atoms available to coordinate with Al and is thus adsorbed on its surface, thus creating a protective layer on its surface that protects the Al against corrosion.

In the case of o-phenylenediamine and hydrazine hydrate has two lone pairs on two NH₂ bonded with an Al, but in the case of o-phenylenediamine a chelate may be formed which stronger than complex formed with open-chain hydrazine hydrate and so Al more easily adsorbed on o-phenylenediamine than that of Hydrazine Hydrate.

Table 2. Inhibition efficiency (% I E) and fractional surface coverage values (θ) use aluminum weight loss method in a 1 M HCl aqueous solution in the absence and existence of different inhibitors (10 mM) for 24 hours.

Inhibitor type	(% I E)	(θ)
2,4-Dinitrophenylhydrazine	88.9%	0.89
o-phenylenediamine	84.7 %	0.85
Hydrazine Hydrate 80 %	77.4	0.77

3.3. Gasometry.

The value of percentage inhibition efficiency (% I E) and the fractional surface coverage values (θ) obtained from the H₂-evolution method for used inhibitors in 1M HCl is summarized in Table 3 using Figures 5 and 6.

Table 3. Output values (% I E) and (θ) of the inhibitors tested in 1M of HCl from measurements of H₂-evolution using Figures 5-6.

Inhibitor type	(% I E)	(θ)
2,4-Dinitrophenylhydrazine	92.6	0.92
o-phenylenediamine	83.8	0.84
Hydrazine Hydrate 80 %	81.8	0.82

The volume of hydrogen produced during aluminum corrosion reaction in 1 M HCl solutions absent of and comprising different inhibitors is calculated as a function of the reaction period, and the results are graphically depicted in Figs. 5 and 6. The inspection of the figures shows that the production of hydrogen begins after the aluminum immersion sheet in the

research solution at a certain duration. This duration can be assumed to equate to the time taken by the acid to dissolve the pre-immersion oxide film prior to the start of the metal attack, which is known as the incubation period. Further examination of the figures shows a linear association in all the solutions evaluated between the reaction time and the volume of hydrogen produced. The involvement of the inhibitor, therefore, reduces the slope of the straight line markedly. Since the line's slope reflects the rate of corrosion reaction, it may be inferred that in the acid solution, the 2, 4-dinitrophenylhydrazine inhibitor has an outstanding potential to inhibit aluminum corrosion. Table 3 displays the values of IEs and the fractional surface coverage values (θ) of the studied inhibitors.

It is evident from the results that the better inhibitor was 2, 4-dinitrophenylhydrazine, and the %IE for compounds investigated decreases in the following order: 2, 4-dinitrophenylhydrazine > o-phenylenediamine > hydrazine hydrate 80 %.

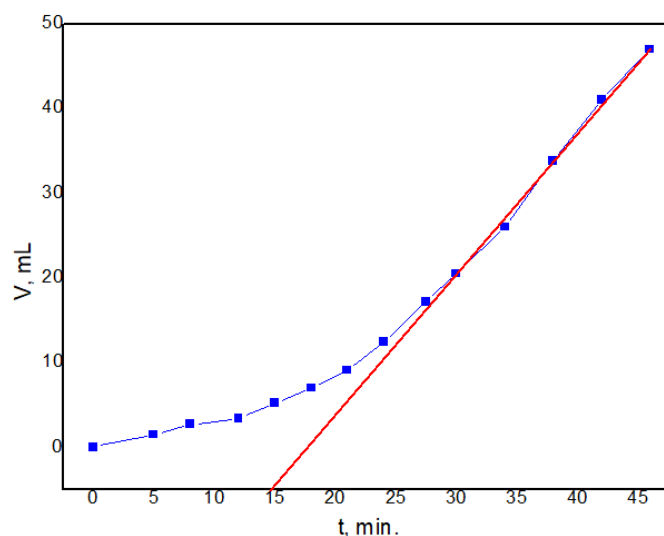


Figure 5. Hydrogen evolution of through aluminum corrosion at 1 M HCl.

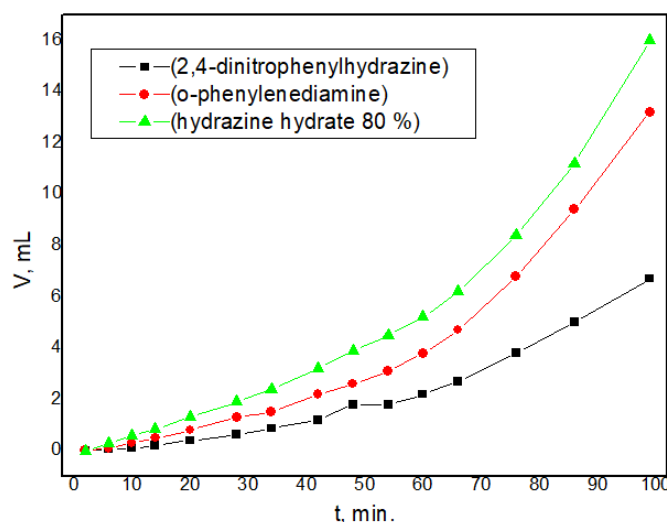


Figure 6. Hydrogen evolution during aluminum corrosion in 1 M HCl in the presence of inhibitors tested (10 mM).

3.4. Effect of the inhibitor concentration (Adsorption Isotherm).

2, 4-dinitrophenylhydrazine inhibitor as an example was used to study the effect of inhibitor concentration by weight loss method. Table 4 summarizes the (% I E) and (θ) values

for various concentrations of 2, 4-dinitrophenylhydrazine inhibitor in 1 M HCl obtained from the weight loss method.

Table 4 indicates that the weight loss reduced and that the reduction of corrosion improved with a rise in the concentration of inhibitor. This phenomenon may be attributed to the fact that as the concentration increases, adsorption and surface coverage increase, and the surface is isolated easily from the liquid. It is obvious that the 2, 4-dinitrophenylhydrazine inhibitor concentration increases the Inhibition efficiency increases.

Table 4. (% I E) and (θ) values utilizing an aluminum weight loss method in a 1 M HCl aqueous solution in the absence and presence of different 2, 4-dinitrophenylhydrazine inhibitor concentrations for 24 hours.

Inhibitor concentration	(% I E)	(θ)
(0.01 M)	88.9	0.89
(0.005 M)	63.7	0.64
(0.0025 M)	40.6	0.41
(0.00125M)	24.3	0.24
(0.000625 M)	13.1	0.13

Adsorption behavior can illustrate the mechanism of corrosion inhibition. Table 4 results are graphically checked by fitting to various isotherms. A $\log \theta$ vs. $\log C$ plot for the inhibitor used (Fig. 7) implies that this compound's adsorption on the surface of Al does not fit the Freundlich adsorption isotherm and that not obeys the relationship: $\log \theta = \log k + 1/n \log C$

Another isotherm tested, and the equation used is the Langmuir Isotherm:

$$C/\theta = 1/K + C \tag{14}$$

Plots of C/θ vs C are shown in Figure 8 for adsorption of the used inhibitor on the aluminum surface in 1 M HCl. The data are showing that this inhibitor is appropriate for Langmuir adsorption isotherm.

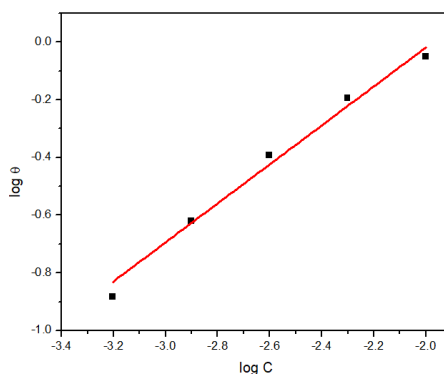


Figure 7. Curve fitting of aluminum corrosion data in 1 M HCl for aluminum in the presence of various concentrations of 2, 4-dinitrophenylhydrazine inhibitor to Freundlich isotherm adsorption.

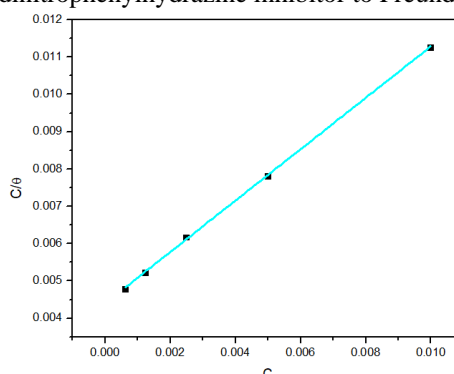


Figure 8. Curve fitting of aluminum corrosion data in 1 M HCl in the presence of different 2, 4-dinitrophenylhydrazine inhibitor concentrations to the Langmuir isotherm adsorption.

3.5. SEM analysis of the metal surface.

Figure 9 (a, b) shows the SEM magnification picture (x 25000) of aluminum immersed in 1 M HCl for 24 hours in the absence and presence of 2, 4-dinitrophenylhydrazine inhibitor. The aluminum surface SEM micrographs in HCl without an inhibitor in Figure 9 (a) show the roughness of the metal surface, indicating Aluminum corrosion in HCl. Figure 9(b) indicates that the surface coverage increases in the presence of 0.5 mM of 2, 4-dinitrophenylhydrazine inhibitor, which in turn results in the formation of the adsorbed compound on the metal surface and the surface is covered by an inhibitor layer that effectively controls the dissolution of aluminum.

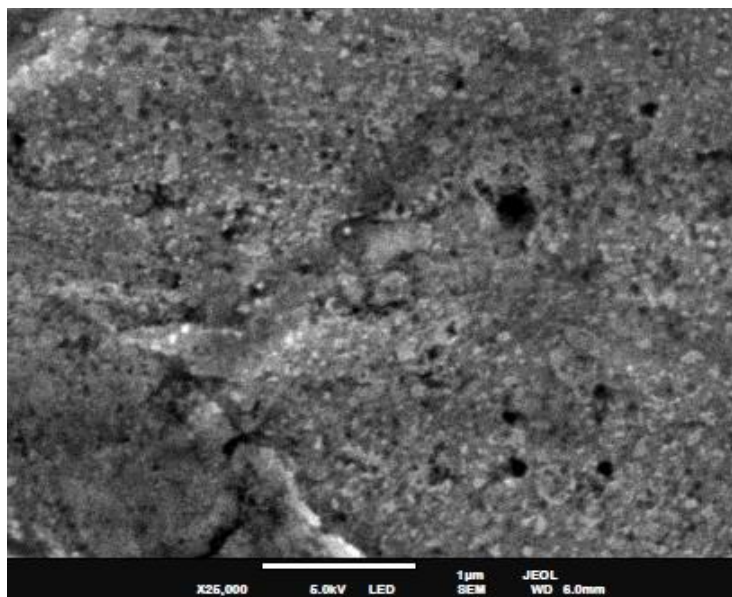


Figure 9a. SEM magnification picture(x 25000) of aluminum immersed in 1 M HCl.

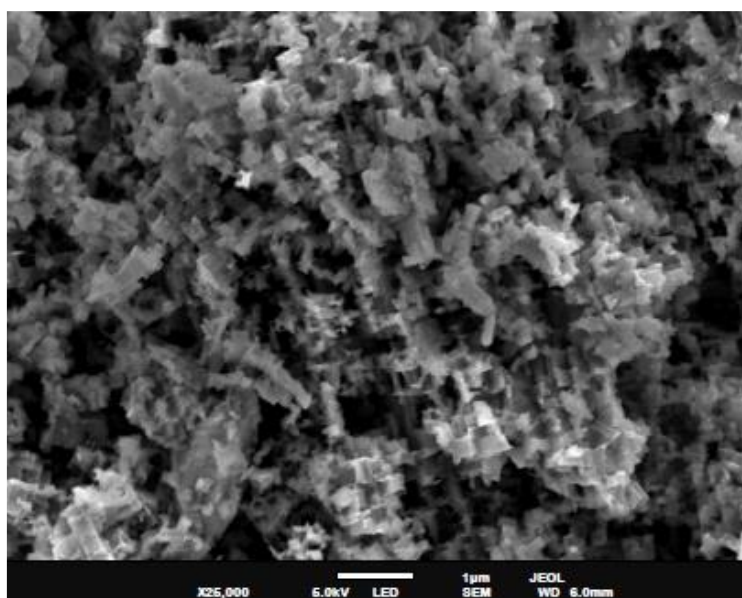


Figure 9b. SEM magnification picture(x 25000) of aluminum immersed in 1 M HCl in the presence of 2, 4-dinitrophenylhydrazine inhibitor.

4. Conclusions

Theoretical DFT calculations were conducted to investigate the reactivity parameters of Amine derivatives related to inhibition efficiency. All quantum chemical parameters describing the inhibition efficiency indicated the high capability of 2, 4-

Dinitrophenylhydrazine as an effective surface coating for metal against corrosion. The obtained theoretical findings were in good accordance with the experimental results. Results obtained from the experimental data shown that Hydrazine Hydrate 80 %, o-phenylenediamine, and (E)-2((2-phenylhydrazono) methyl) phenol act as effective inhibitors of corrosion in HCl acid, but 2,4-Dinitrophenylhydrazine acts as the best one. Corrosion activity was hindered on the aluminum surface by adsorption of organic matter. The studied inhibitors effectively reduced the corrosion rate of aluminum in hydrochloric acid by physically adhering to the corroding metallic surface. The efficacy of the inhibition increases with an increase in o-phenylenediamine concentration. The adsorption of o-phenylenediamine on Aluminum surface from 1M HCl obeys the Langmuir adsorption isotherm. The SEM images demonstrate the construction of the metal surface protective layer. Calculations of gasometric and weight loss inhibition efficiencies are in reasonable approval with one another

Funding

This research received no external funding

Acknowledgments

This research has no acknowledgment.

Conflicts of Interest

The authors declare no conflict of interest.

References

1. Ennouri, A.; Lamiri, A.; Essahli, M. Corrosion Inhibition of Aluminium in Acidic Media by Different Extracts of *Trigonella foenum-graecum* L Seeds. *Portugaliae Electrochimica Acta* **2017**, *35*, 279-295, <https://doi.org/10.4152/pea.201705279>.
2. El-Etre, A.Y. Inhibition of aluminum corrosion using *Opuntia* extract. *Corros. Sci.* **2003**, *45*, 2485-2495, [https://doi.org/10.1016/S0010-938X\(03\)00066-0](https://doi.org/10.1016/S0010-938X(03)00066-0).
3. Müller, B. Corrosion inhibition of aluminium and zinc pigments by saccharides. *Corros. Sci.* **2002**, *44*, 1583-1591, [https://doi.org/10.1016/S0010-938X\(01\)00170-6](https://doi.org/10.1016/S0010-938X(01)00170-6).
4. Assaf F.; Abou-Krishna M.; Yousef T. A.; Abushoffa A.; El-Sheref F.; Toghan A. Influence of Current Density on the Mechanism of Electrodeposition and Dissolution of Zn–Fe–Co Alloys. *Russian Journal of Physical Chemistry* **2020**, *94*, 1708–1715, <https://doi.org/10.1134/S0036024420080026>
5. Hazazi, O.A.; Abdallah, M. Prazole compounds as inhibitors for corrosion of aluminum in hydrochloric acid. *Int. J. Electrochem. Sci* **2013**, *8*, 8138-8152.
6. El-Haddad, M.N.; Fouda, A.S. Electroanalytical, quantum and surface characterization studies on imidazole derivatives as corrosion inhibitors for aluminum in acidic media. *J. Mol. Liq.* **2015**, *209*, 480-486, <https://doi.org/10.1016/j.molliq.2015.06.005>.
7. Hassan, A.T.; Hussein, R.K.; Abou-krisha, M.; Attia, M. Density Functional Theory Investigation of Some Pyridine Dicarboxylic Acids Derivatives as Corrosion Inhibitors. *Int. J. Electrochem. Sci.* **2020**, *15*, 4274-4286, <https://doi.org/10.20964/2020.05.11>.
8. Cang, H.; Fei, Z.; Shao, J.; Shi, W.; Xu, Q. Corrosion inhibition of mild steel by aloe extract in HCl solution medium. *Int. J. Electrochem. Sci.* **2013**, *8*, 720-734.
9. Cohen, S.L.; Brusica, V.A.; Kaufman, F.B.; Frankel, G.S.; Motakef, S.; Rush, B. X-ray photoelectron spectroscopy and ellipsometry studies of the electrochemically controlled adsorption of benzotriazole on copper surfaces. *Journal of Vacuum Science & Technology A* **1990**, *8*, 2417-2424, <https://doi.org/10.1116/1.576708>.
10. Ebenso, E.E.; Eddy, N.O.; Odiongenyi, A.O. Corrosion inhibition and adsorption properties of methocarbamol on mild steel in acidic medium. *Portugaliae Electrochimica Acta* **2009**, *27*, 13-22, <https://doi.org/10.4152/pea.200901013>.
11. Mohamed, M.E.B.; Taha, K.K. Computational Simulation of the Molecular Structure of Benzimidazole and Substituted Benzimidazoles as Corrosion Inhibitors for Brass in Perchloric Acid. *Am. J. Res. Commun.* **2015**.

12. Bhawsar, J.; Jain, P.K.; Jain, P.; Bhawsar, M.R. Computational Study of Corrosion Potential of Ciprofloxacin Drug: DFT Approach. *Asian Journal of Research in Chemistry* **2014**, *7*, 386-389.
13. Peme, T.; Olasunkanmi, L.O.; Bahadur, I.; Adekunle, A.S.; Kabanda, M.M.; Ebenso, E.E. Adsorption and Corrosion Inhibition Studies of Some Selected Dyes as Corrosion Inhibitors for Mild Steel in Acidic Medium: Gravimetric, Electrochemical, Quantum Chemical Studies and Synergistic Effect with Iodide Ions. *Molecules* **2015**, *20*, 16004-16029, <https://doi.org/10.3390/molecules200916004>.
14. Mujica-Martínez, C.A.; Arce, J.C. Mini-bandstructure tailoring in π -conjugated periodic block copolymers using the envelope crystalline-orbital method. *Int. J. Quantum Chem* **2010**, *110*, 2532-2540, <https://doi.org/10.1002/qua.22715>.
15. Mehmeti, V.V.; Berisha, A.R. Corrosion study of mild steel in aqueous sulfuric acid solution using 4-methyl-4H-1, 2, 4-Triazole-3-Thiol and 2-mercaptocotinic acid—an experimental and theoretical study. *Frontiers in chemistry* **2017**, *5*, 61, <https://doi.org/10.3389/fchem.2017.00061>.
16. Anusuya, N.; Sounthari, P.; Saranya, J.; Parameswari, K.; Chitra, S. Quantum chemical study on the corrosion inhibition property of some heterocyclic azole derivatives. *Orient. J.Chem.* **2015**, *31*, 1741–1750, <https://doi.org/10.13005/ojc/310355>.
17. Al-Amiery, A.; Salman, T.A.; Alazawi, K.F.; Shaker, L.M.; Kadhum, A.A.H.; Takriff, M.S. Quantum chemical elucidation on corrosion inhibition efficiency of Schiff base: DFT investigations supported by weight loss and SEM techniques. *International Journal of Low-Carbon Technologies* **2020**, *15*, 202-209, <https://doi.org/10.1093/ijlct/ctz074>.
18. Chaouiki, A.; Lgaz, H.; Salghi, R.; Gaonkar, S.L.; Bhat, S.; Jodeh, S.; Toumiat, K.; Oudda, H. New benzohydrazide derivative as corrosion inhibitor for carbon steel in a 1.0 M HCl solution: electrochemical, DFT and Monte Carlo simulation studies. *Portugaliae Electrochimica Acta* **2019**, *37*, 1-9 <https://doi.org/10.4152/pea.201903147>.
19. El-Mansy M. A.M.; Osman O.; Mahmoud A. A.; Elhaes H.; Gawad A. E. A.; Ibrahim M. A. Computational Notes on the Chemical Stability of Flutamide. *Letters in Applied NanoBioScience* **2020**, *9*, 1147 – 1155, <https://doi.org/10.33263/LIANBS93.11471155>.
20. Fouda A. E. S.; Rashwan S. M.; Kamel M. M.; Abdel Haleem E. Chemical, electrochemical and surface morphology investigation of Cichorium intybus extract (CIE) as beneficial inhibitor for Al in 2 M HCl acid *Letters in Applied NanoBioScience* **2020**, *9*(2), 1064 – 1073, <https://doi.org/10.33263/LIANBS92.10641073>.
21. Diki N.; Silvère Y.; Valery B.K.; Guy-richard M.; Augustin O. Cefadroxil Drug as Corrosion Inhibitor for Aluminum in 1 M HCl Medium: Experimental and Theoretical Studies. *IOSR Journal of Applied Chemistry* **2018**, *11*, 24–36, <https://doi.org/10.9790/5736-1104012436>.
22. Udensi, S.C.; Ekpe, O.E.; Nnanna, L.A. Newbouldia laevis Leaves Extract as Tenable Eco-Friendly Corrosion Inhibitor for Aluminium Alloy AA7075-T7351 in 1 M HCl Corrosive Environment: Gravimetric, Electrochemical and Thermodynamic Studies. *Chemistry Africa* **2020**, *3*, 303-316, <https://doi.org/10.1007/s42250-020-00131-w>.
23. Nnaji, N.; Nwaji, N.; Mack, J.; Nyokong, T. Corrosion Resistance of Aluminum against Acid Activation: Impact of Benzothiazole-Substituted Gallium Phthalocyanine. *Molecules* **2019**, *24*, 207, <https://doi.org/10.3390/molecules24010207>.
24. Musa, A.Y.; Kadhum, A.A.H.; Mohamad, A.B.; Takriff, M.S. Experimental and theoretical study on the inhibition performance of triazole compounds for mild steel corrosion. *Corros. Sci.* **2010**, *52*, 3331-3340, <https://doi.org/10.1016/j.corsci.2010.06.002>.
25. Moretti, G.; Guidi, F.; Fabris, F. Corrosion inhibition of the mild steel in 0.5M HCl by 2-butyl-hexahydropyrrolo[1,2-b][1,2]oxazole. *Corros. Sci.* **2013**, *76*, 206-218, <https://doi.org/10.1016/j.corsci.2013.06.044>.
26. Becke, A.D. A new mixing of Hartree–Fock and local density-functional theories. *The Journal of Chemical Physics* **1993**, *98*, 1372-1377, <https://doi.org/10.1063/1.464304>.
27. Lee, C.; Yang, W.; Parr, R.G. Development of the Colle-Salvetti correlation-energy formula into a functional of the electron density. *Physical review B* **1988**, *37*, 785, <https://doi.org/10.1103/PhysRevB.37.785>.
28. Ebenso, E.E.; Arslan, T.; Kandemirli, F.; Caner, N.; Love, I. Quantum chemical studies of some rhodanine azosulpha drugs as corrosion inhibitors for mild steel in acidic medium. *Int. J. Quantum Chem* **2010**, *110*, 1003-1018, <https://doi.org/10.1002/qua.22249>.
29. Neese, F. Software update: the ORCA program system, version 4.0. *Wiley Interdisciplinary Reviews: Computational Molecular Science* **2018**, *8*, e1327, <https://doi.org/10.1002/wcms.1327>.
30. Hanwell, M.D.; Curtis, D.E.; Lonie, D.C.; Vandermeersch, T.; Zurek, E.; Hutchison, G.R. Avogadro: an advanced semantic chemical editor, visualization, and analysis platform. *J. Cheminform.* **2012**, *4*, 17, <https://doi.org/10.1186/1758-2946-4-17>.
31. Pérez, P.; Contreras, R.; Vela, A.; Tapia, O. Relationship between the electronic chemical potential and proton transfer barriers. *Chem. Phys. Lett.* **1997**, *269*, 419-427, [https://doi.org/10.1016/S0009-2614\(97\)00313-8](https://doi.org/10.1016/S0009-2614(97)00313-8).
32. Geerlings, P.; De Proft, F.; Langenaeker, W. Conceptual Density Functional Theory. *Chem. Rev.* **2003**, *103*, 1793-1874, <https://doi.org/10.1021/cr990029p>.

33. Ayawei, N.; Ebelegi, A.N.; Wankasi, D. Modelling and interpretation of adsorption isotherms. *Journal of Chemistry* **2017**, *2017*, <https://doi.org/10.1155/2017/3039817>.
34. Yousef, T.A. Structural, optical, morphology characterization and DFT studies of nano sized Cu(II) complexes containing schiff base using green synthesis. *J. Mol. Struct.* **2020**, *1215*, 128180, <https://doi.org/10.1016/j.molstruc.2020.128180>.
35. Yousef, T.A.; Hussein, R.K.; Abou-krissha, M. DFT investigation of geometrical structure, IR and RAMAN spectra of vinyl halides CH₂=CH-X (X IS F, Cl AND Br). *International Journal of Pharmaceutical Sciences and Research* **2019**, *10*, 5537-5544, [https://doi.org/10.13040/IJPSR.0975-8232.10\(12\).5537-44](https://doi.org/10.13040/IJPSR.0975-8232.10(12).5537-44).
36. Mourya, P.; Singh, P.; Tewari, A.K.; Rastogi, R.B.; Singh, M.M. Relationship between structure and inhibition behaviour of quinolinium salts for mild steel corrosion: Experimental and theoretical approach. *Corros. Sci.* **2015**, *95*, 71-87, <https://doi.org/10.1016/j.corsci.2015.02.034>.
37. Kosari, A.; Moayed, M.H.; Davoodi, A.; Parvizi, R.; Momeni, M.; Eshghi, H.; Moradi, H. Electrochemical and quantum chemical assessment of two organic compounds from pyridine derivatives as corrosion inhibitors for mild steel in HCl solution under stagnant condition and hydrodynamic flow. *Corros. Sci.* **2014**, *78*, 138-150, <https://doi.org/10.1016/j.corsci.2013.09.009>.
38. Behpour, M.; Ghoreishi, S.M.; Khayatkashani, M.; Soltani, N. The effect of two oleo-gum resin exudate from *Ferula assa-foetida* and *Dorema ammoniacum* on mild steel corrosion in acidic media. *Corros. Sci.* **2011**, *53*, 2489-2501, <https://doi.org/10.1016/j.corsci.2011.04.005>.
39. Parr, R.G.; Pearson, R.G. Absolute hardness: companion parameter to absolute electronegativity. *J. Am. Chem. Soc.* **1983**, *105*, 7512-7516, <https://doi.org/10.1021/ja00364a005>.
40. Huang, W.; Tan, Y.; Chen, B.; Dong, J.; Wang, X. The binding of antiwear additives to iron surfaces: quantum chemical calculations and tribological tests. *Tribology International* **2003**, *36*, 163-168, [https://doi.org/10.1016/S0301-679X\(02\)00130-5](https://doi.org/10.1016/S0301-679X(02)00130-5).
41. Herrag, L.; Hammouti, B.; Elkadiri, S.; Aouniti, A.; Jama, C.; Vezin, H.; Bentiss, F. Adsorption properties and inhibition of mild steel corrosion in hydrochloric solution by some newly synthesized diamine derivatives: Experimental and theoretical investigations. *Corros. Sci.* **2010**, *52*, 3042-3051, <https://doi.org/10.1016/j.corsci.2010.05.024>.
42. Lukovits, I.; Kalman, E.; Zucchi, F. Corrosion inhibitors—correlation between electronic structure and efficiency. *Corrosion* **2001**, *57*, 3-8, <https://doi.org/10.5006/1.3290328>.